Softened zone formation and joint strength properties in dissimilar friction welds

C. MALDONADO
Instituto de Investigaciones Metalúrgicas Universidad Michoacana de San Nicolás de Hidalgo, Morelia, Mich., Mexico
E-mail: cmzepeda@zeus.umich.mx

T. H. NORTH
Department of Metallurgy & Materials Science, University of Toronto, Toronto, Ont., Canada

The mechanical properties of dissimilar MMC/AISI 304 stainless steel friction welds with and without silver interlayers were examined. The notch tensile strengths of MMC/AISI 304 stainless steel and MMC/Ag/AISI 304 stainless steel friction welds increased when high friction pressures were applied during the joining operation. The higher notch tensile strengths of dissimilar MMC/AISI and MMC/Ag/AISI 304 stainless steel friction welds resulted from the formation of narrow softened zones in MMC material immediately adjacent to the bondline. The influence of softened zone width and hardness (yield strength) on the notch tensile strengths of dissimilar welds was analysed using finite element modelling (FEM). FEM in combination with the assumption of a ductile failure criterion was used to calculate the notch tensile strengths of dissimilar joints. The key assumption in this work is that dissimilar weld failure wholly depended on the characteristics (mechanical properties and dimensions) of the softened zone formed in MMC material immediately adjacent to the bondline. The modelling results produced based on this assumption closely correspond with the actual notch tensile strengths of dissimilar MMC/Ag/AISI 304 stainless steel and MMC/Ag/AISI 304 stainless steel friction welds. © *2002 Kluwer Academic Publishers*

1. Introduction

Friction welding provides a straightforward and highly controllable means of joining dissimilar metal substrates. However, much prior research has indicated that the mechanical properties of completed joints are largely determined by the formation of intermetallic layers at the dissimilar joint interface. For example, FeAl, Fe_2Al_5, and Fe_4Al_3 formation have been confirmed at the bondline of dissimilar Al 6061-T6 10 vol% Al_2O_3/AISI 304 stainless steel friction welds [1]. It has been suggested that the mechanical properties of dissimilar friction welds are markedly decreased when a critical intermetallic layer width is exceeded [2–4]. However, in addition to intermetallic layer formation, the friction welding operation also produces other metallurgical changes in the heat-affected zone, changes that also have a markedly detrimental effect on the mechanical properties of completed welds. In particular, softened zones are formed adjacent to the bondline when age-strengthened aluminium alloys are friction welded. The formation of wide softened regions adjacent to the bondline have been associated with low notch tensile strength properties in Al 6061 T6/Al 6061 T6 and Al 6061 T6 MMC/Al 6061 T6 MMC welds [5]. With this in mind, the mechanical properties of dissimilar welds involving age-strengthened aluminium alloys will be determined by both intermetallic layer formation and on the presence of softened regions adjacent to the bondline.

The present paper examines the mechanical properties of dissimilar Al 6061-T6 10 vol% Al_2O_3/AISI 304 stainless steel and Al 6061-T6 10 vol% Al_2O_3/Ag/AISI 304 stainless steel friction welds produced using a range of friction pressures. In the present paper, the influence of softened zones on joint mechanical properties is evaluated using finite element modelling. Almond *et al.* [5] previously used finite element modelling when they investigated the tensile strengths of brazed steel/Cu/steel joints. The stress and strain distributions in the copper interlayer were calculated using FEM analysis and satisfactorily predicted the stress/strain relations in joints that had different interlayer thickness/diameter ratios [6]. Also, Henshall *et al.* [7] used FEM when examining the mechanical properties of brazed dissimilar AISI 304/Ag/AISI 304 stainless steel joints. Although they suggested that finite element method could be used to calculate the final strength of brazed joints they did not suggest a failure criterion that could be used to accomplish this task. For these reason, FEM modelling is used in the present study to investigate the mechanical behaviour of dissimilar Al 6061-T6 10 vol% Al_2O_3/AISI 304 stainless steel friction welds produced with and

TABLE I Chemical composition of materials (wt%)

MMC	Al	Mg	Si	C	Cu	Fe	Zn
	97.76	1.15	0.535	0.099	0.225	0.121	0.022
AISI 304	C	Si	Mn	Ni	Cr	Mo	V
	0.040	0.006	1.15	9.5	17.9	0.540	0.08

without silver interlayers. It is confirmed in this work that the tensile strength properties of dissimilar friction welds can be satisfactorily calculated by assuming that they are wholly determined by the yield strength and dimensions of the softened zone produced adjacent to the dissimilar joint interface.

2. Experimental procedure

2.1. Materials

All dissimilar friction welds were made using 19-mm bars of Al 6061-T6 base material containing 10 vol% of reinforcing Al_2O_3 particles. The MMC base material displayed some evidence of particle clustering and had a banded morphology as a result of particle alignment and agglomeration that occurred during processing. This created a slightly inhomogeneous and anisotropic composite base material. The chemical compositions of the MMC and AISI 304 stainless steel base materials are indicated in Table I. For simplicity the Al 6061-T6 10 vol%Al_2O_3 material will be referred to as MMC base material and dissimilar welds with and without silver interlayers will be referred to as MMC/AISI 304 stainless steel or MMC/Ag/AISI 304 stainless steel joints.

Silver interlayers were electrodeposited onto the stainless steel substrate, which had been previously coated with a nickel strike layer. The nickel strike served as a base for subsequent silver coating; this approach has been applied previously during both dissimilar friction welding and dissimilar diffusion bonding investigations [8–10]. The electroplating procedure [10] comprised surface degreasing and cleaning in 10 vol% NaOH for 2 minutes, followed by deposition of an 8 μm thick nickel barrier layer in a nickel chloride bath for 5 minutes. The current density was 538 A/m^2, the bath temperature was 25°C and the plating time was 20 minutes in a silver potassium cyanide plating solution. The current density was 50 A/m^2 and the average thickness of the silver interlayer was 20 μm.

The contacting surfaces of the stainless steel and MMC substrates were machined perpendicular to the longitudinal axis of the as-received bar. The stainless steel sections were polished using 1 μm diamond paste prior to friction joining while the MMC substrate was polished using 1200 grade emery paper. Prior to friction welding, the electroplated stainless steel and the MMC sections were cleaned using acetone. Adhesion between the nickel barrier layer and the stainless steel substrate substrates was improved via vacuum heat treatment of the electroplated stainless steel samples at 650°C for 1 hour and at 800°C for 15 minutes [11]. The microstructure of an MMC/AISI 304 stainless steel friction weld containing a silver interlayer and nickel barrier is shown in Fig. 1.

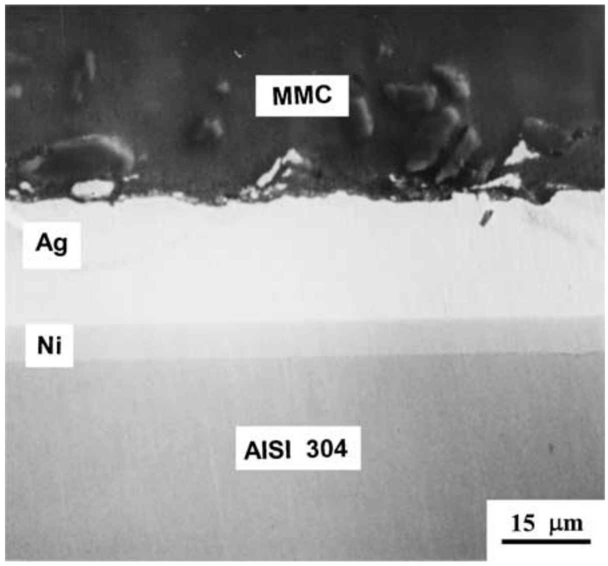

Figure 1 Secondary electron SEM micrograph showing the silver interlayer at the bondline of dissimilar MMC/Ag/AISI 304 stainless steel friction joints.

2.2. Welding procedure

All welds were produced using a continuous-drive machine rated at 15 kW transmission power with a maximum axial thrust of 110 KN. The friction pressure (P1) was varied from 30 MPa to 240 MPa with the rotational speed held constant at 1500 rpm. The forging pressure and forging time were 240 MPa and 1.0 s respectively.

Fig. 2 shows the design of the notch tensile test specimen employed when examining the mechanical properties of dissimilar friction welds. The tensile strengths of the as-received MMC and AISI 304 stainless steel base materials were evaluated using standard round tension test specimens. The aluminium alloy material was tested following the ASTM B 557M standard, while the stainless steel material was tested using following the ASTM A 370 standard. Table II shows the mechanical properties of the as-received materials. The dimensions of the softened zones formed in the aluminium-based MMC substrate were measured from microhardness traverses made using a 100 g load, with all hardness traverses being made at the component half radius.

2.3. Finite element modelling

Commercial software (ANSYS 5.5^{TM}) was used when modelling the mechanical situation in notch tensile

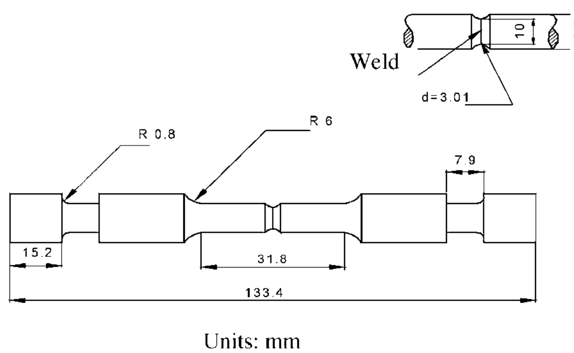

Figure 2 U-notch tensile testing specimen configuration.

TABLE II Mechanical properties of materials

Material	Ultimate tensile strength (MPa)	Yield strength (MPa)	Elongation (%)	E (GPa)	Poisson's ratio (ν)
MMC	322	290	7.9	81.4	0.332
AISI 304	698	333	69	196	0.3

specimens extracted from dissimilar friction welds. All calculations were performed using triangular 6-node elements. The geometry and meshing of the finite element model are shown in Fig. 3A and B. A two dimensional analysis of one half of the specimen was employed because of the axy-symmetrical shape of the notch tensile test specimen. The left-hand edge in Fig. 3A (at $r = 0$) corresponds with the central axis of the notch tensile specimen. The mesh contained 2257 elements and 4694 nodes and at $r = 0$, the nodes were allowed to move only in the axial direction. The bottom edge was fixed at $z = -15$ mm and the axial displacement, $U_Z = 0$. Simulated tensile loads were applied at $z = +15$ mm during FEM modelling, with the applied stress continuously increasing with time from 0 to 400 MPa.

Elastic behaviour was represented using linear isotropic elasticity theory, while time-independent plastic deformation was represented using isotropic Von Mises plasticity theory. Both base materials (MMC and AISI 304 stainless steel) were assumed to behave as bi-linear kinematic hardening materials.

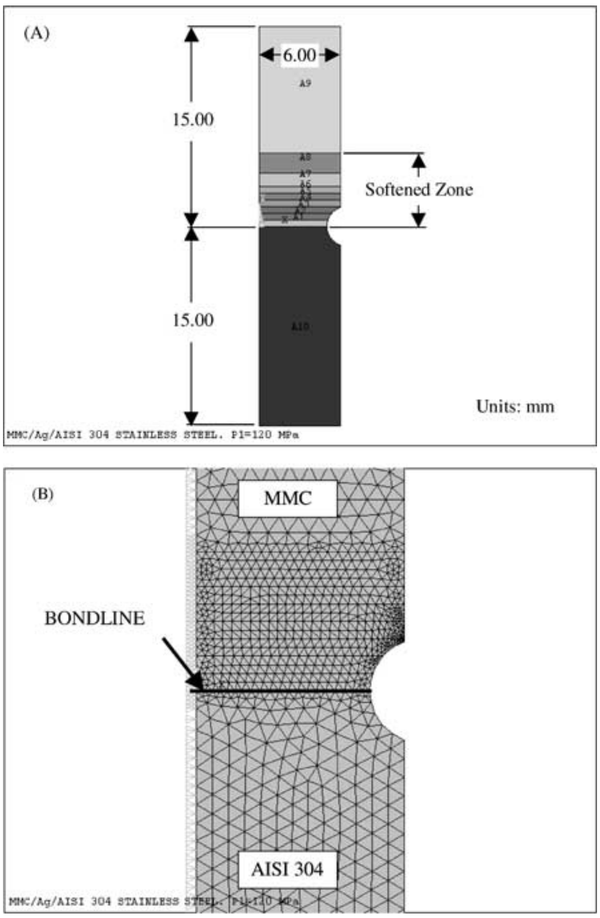

Figure 3 (A) Half of the notch tensile specimen. (B) Finite element idealisation of the notch tensile specimen.

3. Results

3.1. Joint mechanical properties

Fig. 4 shows the relation between friction pressure and the notch tensile strengths of dissimilar MMC/Ag/AISI 304 stainless steel and MMC/AISI 304 stainless steel welds. During these tests, all other welding parameters (friction time, rotational speed, forging pressure, and forging time) were held constant. Higher notch tensile strengths were produced when increased friction pressures were applied during MMC/Ag/AISI 304 stainless steel and MMC/AISI 304 stainless steel welding. The effective plastic strain measured on the fractured section of the tensile test specimen in the MMC substrate was also higher in dissimilar joints produced using silver interlayers. The effective plastic strain produced during notch tensile sample failure was evaluated using Equation 1 [11, 12]:

$$\bar{\varepsilon}_{\mathrm{p}} = 2 \ln \left(\frac{d_{\mathrm{o}}}{d} \right) \quad (1)$$

where $\bar{\varepsilon}_{\mathrm{p}}$ = the effective plastic strain; d_{o} = the original specimen diameter; d = the final diameter of the specimen at the neck.

The effective plastic strain increased from 0.25% to 5.0% in dissimilar MMC/Ag/AISI 304 stainless steel friction welds and from 0.1% to 0.25% in dissimilar MMC/AISI 304 stainless steel friction welds when the friction pressure increased from 30 to 240 MPa (see Fig. 5).

Quite different failure modes were observed in MMC/Ag/AISI 304 stainless steel friction welds. Failure in MMC/Ag/AISI 304 stainless steel welds produced using a low friction pressure (30 MPa) occurred via a combination of brittle, interfacial and ductile fracture, i.e. brittle failure through regions containing Ag_3Al, interfacial failure at the silver/aluminium interface, and ductile fracture through the MMC base material. However, when the friction pressure was raised to 240 MPa the failure mode was wholly ductile through the MMC base material. In dissimilar MMC/AISI 304

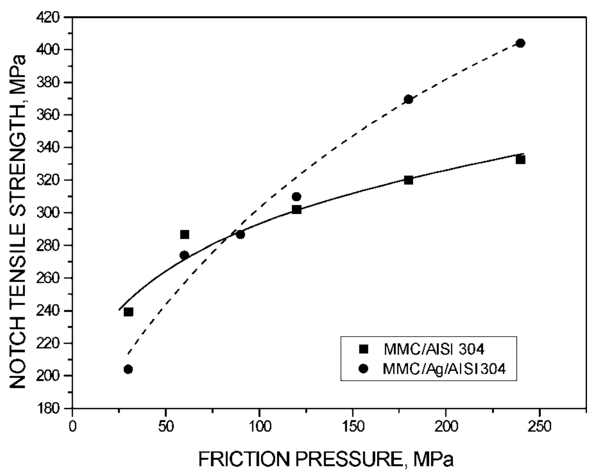

Figure 4 Influence of friction pressure on the notch tensile strength of MMC/AISI 304 and MMC/Ag/AISI 304 stainless steel friction joints. Friction time, 4s; forging pressure, 240 MPa; forging time, 1s.

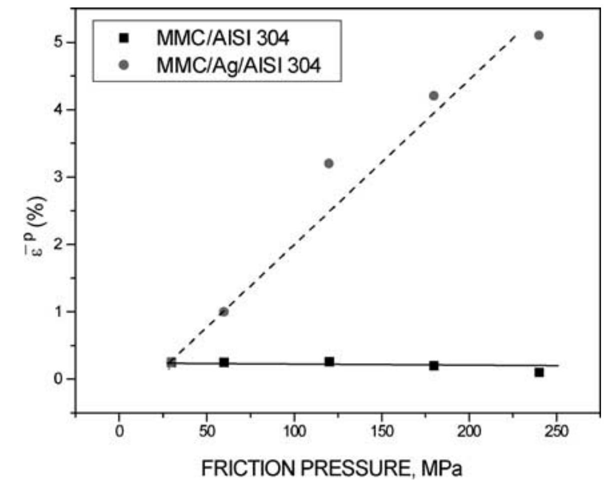

Figure 5 Relationship between the effective plastic strain and the notch tensile strengths of MMC/AISI 304 and MMC/Ag/AISI 304 stainless steel friction joints. Friction time, 4 s; forging pressure, 240 MPa; forging time, 1 s.

stainless steel friction welds produced using a friction pressure of 30 MPa, failure resulted from a combination of ductile and brittle failure. Brittle failure became the dominant mode of fracture when the friction pressure increased from 30 MPa to 240 MPa [14].

In the present research, the softened zone is the region extending from the bondline to the location where the MMC material reaches a hardness of 117.5 HV, this is the hardness value of the MMC base material prior to

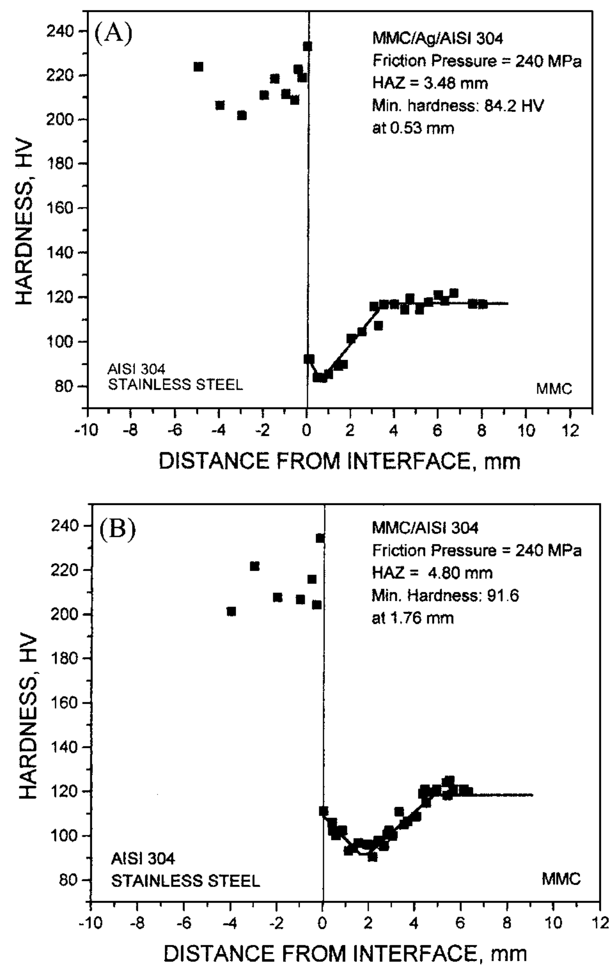

Figure 6 Vickers hardness distribution across the joint interface. Friction pressure, 240 MPa; friction time, 4 s; forging pressure, 240 MPa; forging time, 1 s.

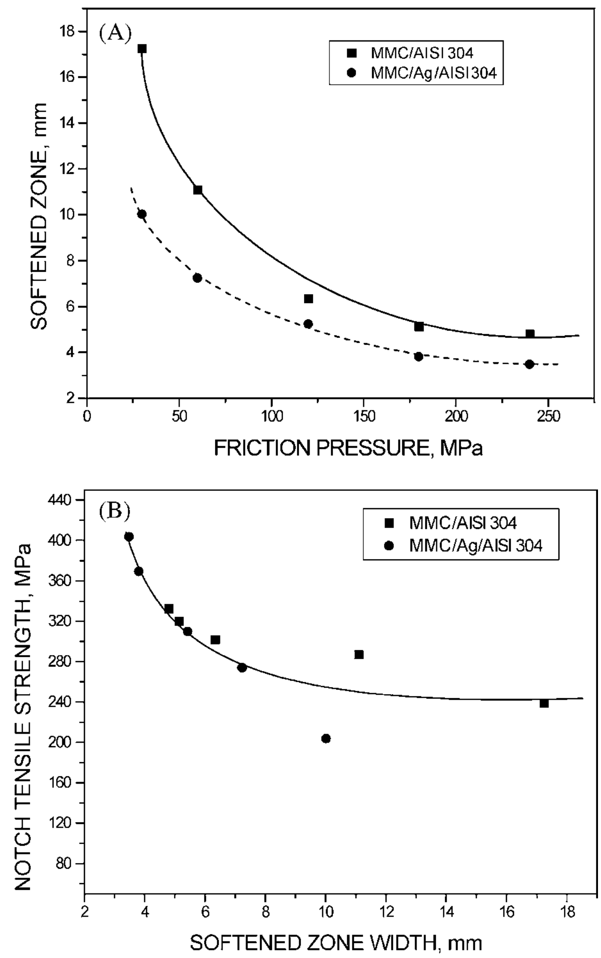

Figure 7 (A) Influence of friction pressure on the softened zone width and (B) Relation between softened zone width and the notch tensile strengths of dissimilar MMC/AISI 304 and MMC/Ag/AISI 304 stainless steel friction joints. Friction time, 4 s; forging pressure, 240 MPa; forging time, 1 s; rotational speed, 1500 rpm.

the friction welding operation, Fig. 6 shows the hardness distribution of dissimilar MMC/Ag/AISI 304 and MMC/AISI 304 friction welds produced with a friction pressure of 240 MPa. Fig. 7A shows that the widths of the softened zone decreased in welds made using high friction pressures. The relation between softened zone width and the notch tensile strength properties is shown in Fig. 7B.

The mechanical properties of MMC base material immediately adjacent to the bondline have a critical influence on the tensile strength of dissimilar joints. The hardness measurements close to the bondline are affected by the steel substrate, for this reason, the microhardness values at the location 0.125 mm from the dissimilar joint interface were considered to be representative of the mechanical properties of MMC material adjacent to the bondline. Fig. 8A shows the relation between friction pressure and microhardness values at this location in completed welds, while Fig. 8B shows the relation between notched tensile strength and the hardness of the softened region. Higher hardness values were found in dissimilar friction welds produced using high friction pressures.

3.2. Finite element modeling results

The mechanical properties of MMC base material in the softened zone immediately adjacent to the dissimilar

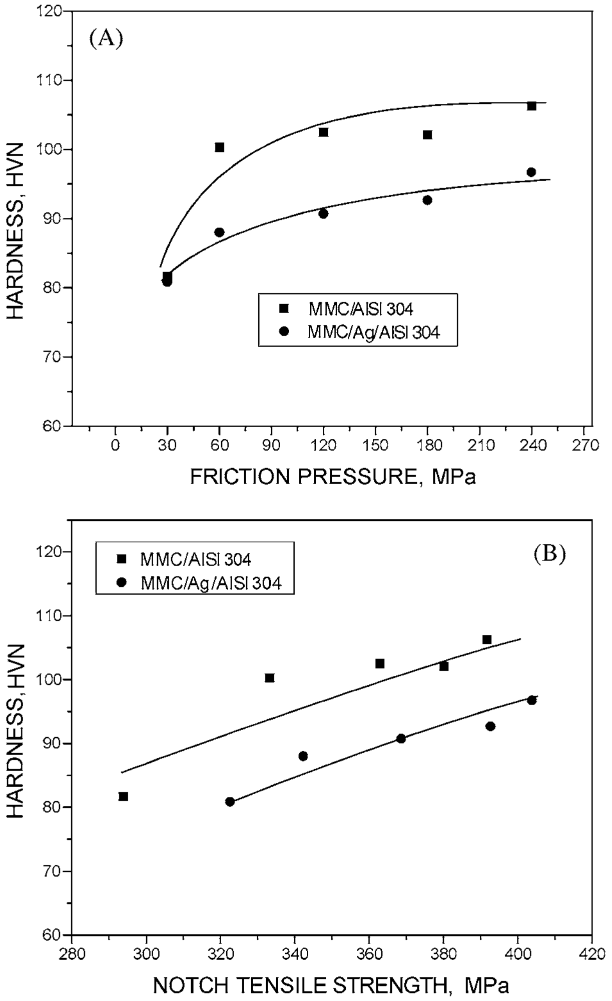

Figure 8 (A) Influence of friction pressure on the hardness of the adjoining MMC substrate. (B) Relationship between the hardness of the adjoining MMC substrate and the notch tensile strengths of dissimilar MMC/AISI 304 stainless steel and MMC/Ag/AISI 304 stainless steel friction joints. All hardness measurements at the located at 0.125 mm from the bondline. Friction time, 4 s; forging pressure, 240 MPa; forging time, 1 s; rotational speed, 1500 rpm.

joint interface were calculated using Equations 2 and 3:

$$\sigma_y(\text{MPa}) = 3.0HVN - 58.5 \qquad (2)$$

$$\sigma_T(\text{MPa}) = 2.8HVN + 16.5 \qquad (3)$$

These equations are adapted to the current MMC base material of the regression relations developed by Myhr and Grong [15] and relate microhardness values with yield and tensile strength properties. The unnotched failure stress (σ_{UF}) was assumed to be equal to the tensile strength of the as-received metal matrix composite material.

Microhardness traverse results are transformed into yield strength values using Equation 2. Since the assumption was made that the MMC and the stainless steel substrates behave as bilinear kinematic materials, the value of the tangential modulus in the softened zone (E_T) equalled the tangential modulus of the MMC base material prior to friction welding. This assumption is supported by the results produced by Hval *et al.* [16] showing that the tangential modulus was unchanged when the yield strength of simulated softened regions increased in aluminium alloy Al 6083 base material. The tangential modulus (E_T) value was calculated by combining Equation 4 with the stress/strain output produced during mechanical testing of as-received MMC and AISI 304 stainless steel base materials:

$$\hat{\sigma}_E = \sigma_y + \frac{E E_T}{E - E_T}\hat{\varepsilon} \qquad (4)$$

where, $\hat{\sigma}_E$ = equivalent plastic stress, σ_y = yield strength, E = Young's modulus, E_T = tangential modulus, $\hat{\varepsilon}$ = equivalent plastic strain.

For a true strain of 0.1 the tangential moduli for the MMC and stainless steel substrates are 375 MPa and 2260 MPa respectively.

The effects of the softened zone formation on the equivalent (Von Mises) stress, the total equivalent strain and the triaxiality factor are evaluated along lines parallel to the dissimilar joint interface. The calculated results are expressed as function of the r/a ratio, where r is the radial distance measured from the centreline of the tensile test specimen to the location considered and a is the sample radius in the notch region.

The equivalent stress distribution in dissimilar MMC/AISI 304 welds is evaluated along a horizontal line located at a distance of 1 mm from the joint interface when an applied stress of 160 MPa is assumed during FEM modelling. Fig. 9A indicates that the equivalent stress for r/a values from 0 to 0.8 is much lower in MMC/AISI 304 stainless steel welds made using high friction pressures (240 MPa). In the MMC/AISI 304 stainless steel welds produced using a friction pressure of 30 MPa the equivalent stress (191.32 MPa)

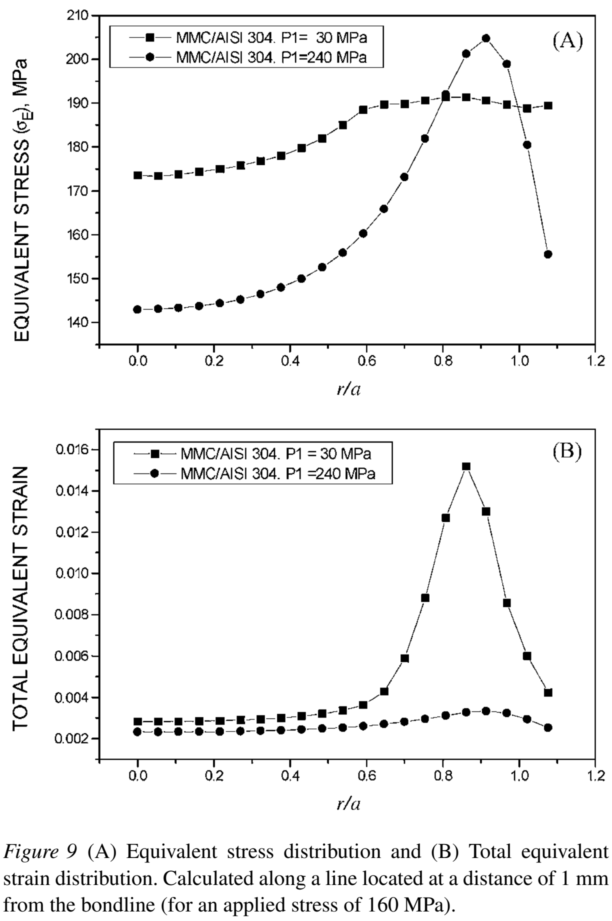

Figure 9 (A) Equivalent stress distribution and (B) Total equivalent strain distribution. Calculated along a line located at a distance of 1 mm from the bondline (for an applied stress of 160 MPa).

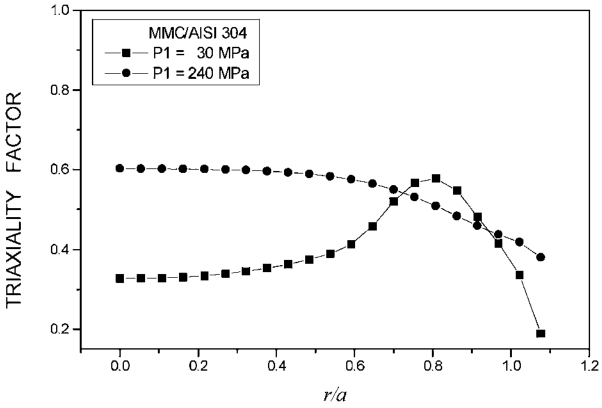

Figure 10 Triaxiality factor distribution on a line located at a distance of 1 mm from the bondline in MMC/AISI 304 stainless steel friction joints. For an applied stress = 160 MPa.

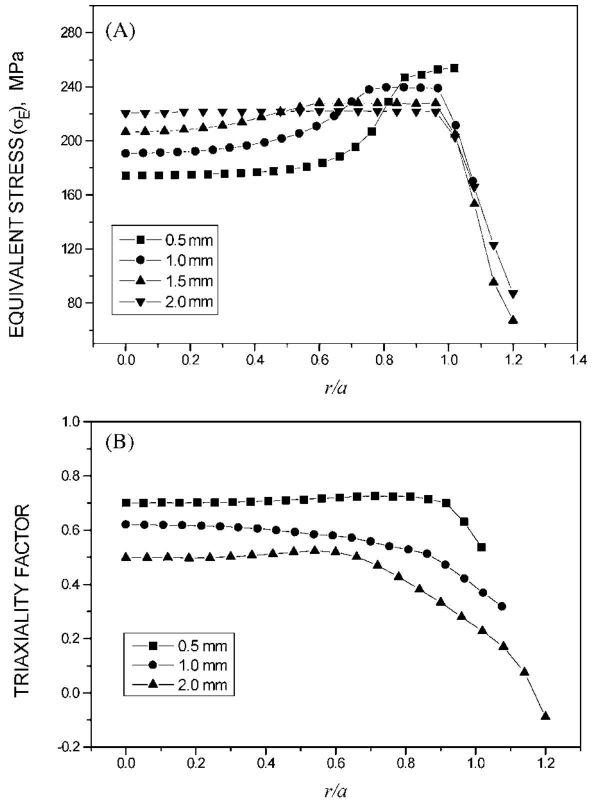

Figure 11 (A) Equivalent stress distribution and (B) Triaxiality factor distribution along lines parallel to the bondline in a dissimilar MMC/AISI 304 stainless steel friction joint. P1 = 240 MPa and softened zone width = 4.80 mm. For an applied pressure = 200 MPa.

exceeds the calculated yield strength (180.6 MPa) at $r/a = 0.85$. The softened zone is therefore plastically deformed at this location (see Fig. 9B). In contrast, in dissimilar MMC/AISI 304 welds produced using high friction pressures (240 MPa), an applied stress exceeding 160 MPa is needed to produce yielding at a similar location.

The highest triaxiality factor occurs at the joint centreline in dissimilar MMC/AISI 304 stainless steel welds produced using a friction pressure of 240 MPa, see Fig. 10. In contrast, the peak triaxiality factor value occurs at $r/a = 0.81$ in MMC/AISI 304 stainless steel welds produced using a low friction pressure (30 MPa).

Fig. 11A shows the equivalent stresses acting on lines located at 0.5 mm, 1 mm, 1.5 mm and 2 mm from the dissimilar joint interface in a MMC/AISI 304 stainless steel friction weld made using a friction pressure of 240 MPa. On the line located 0.5 mm from the bondline the peak equivalent stress occurs at the specimen periphery. However, at increasing distances from the bondline the peak equivalent stress shifts towards the centreline of the tensile test specimen. Fig. 11B shows that the highest triaxiality factors are produced in regions close to the joint interface at the sample centerline. Lower triaxiality factors are found close to the periphery of the tensile test specimen. Similar changes in the location of the peak stress were found when dissimilar maraging steel/Ag/maraging steel joints were modelled [17].

3.2.1. Calculating notch tensile strength

The notch acts as a stress concentrator during notch tensile testing and produces localised plastic deformation in material located at the notch root. For this reason a triaxiality factor is required and this depends on the relation:

$$\text{triaxiality factor} = \frac{\sigma_m}{\sigma_E} \tag{5}$$

where, σ_m is the average stress given by,

$$\sigma_m = \frac{\sigma_1 + \sigma_2 + \sigma_3}{3} \tag{6}$$

and σ_1, σ_2, and σ_3 are principal stresses. The equivalent stress (σ_E) is calculated from the relation:

$$\sigma_E = \frac{\sqrt{2}}{2}\left[(\sigma_1-\sigma_2)^2+(\sigma_2-\sigma_3)^2+(\sigma_3-\sigma_1)^2\right]^{1/2} \tag{7}$$

The triaxiality factor has a value of 1/3 at the periphery of notched tensile test specimens and has a maximum value at the notch centreline [12, 13]. The maximum value of the triaxiality factor is determined by the relation:

$$\left(\frac{\sigma_m}{\sigma_E}\right)_{MAX} = \frac{1}{3} + \ln\left(\frac{a}{2R} + 1\right) \tag{8}$$

where, $a = d/2$ is the radius of the minimum cross-section of the notched specimen, R = the profile radius of the notched specimen.

Although, Equation 8 can be used to calculate the maximum triaxiality factor in homogeneous specimens, it cannot be applied to dissimilar MMC/AISI 304 stainless steel friction joints since the mechanical properties of the MMC and AISI 304 stainless steel substrates are markedly different. Also, the softened zone formed in MMC base material adjacent to the dissimilar joint interface will make the analytical situation even more complex. With this in mind, the mechanical heterogeneity (strength mis-match) during failure of notched tensile specimens from dissimilar friction welds was investigated using FEM. However, although FEM modelling allows determination of stress and strain distributions in notch tensile specimens, it does not indicate the applied

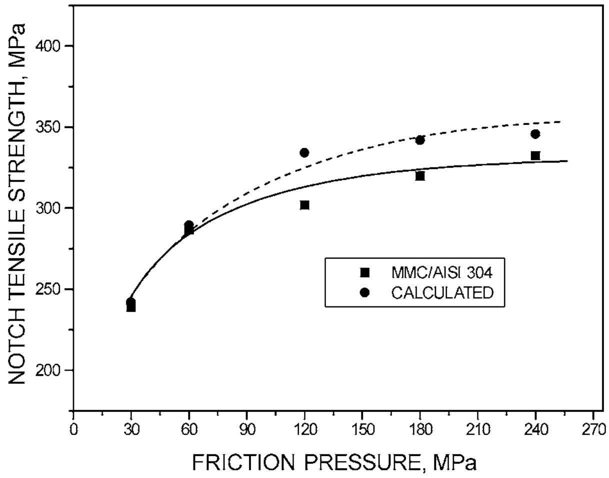

Figure 12 Calculated and actual notch tensile strengths in dissimilar MMC/AISI 304 stainless steel friction joints. Friction time, 4 s; forging pressure, 240 MPa; forging time, 1 s; rotational speed, 1500 rpm.

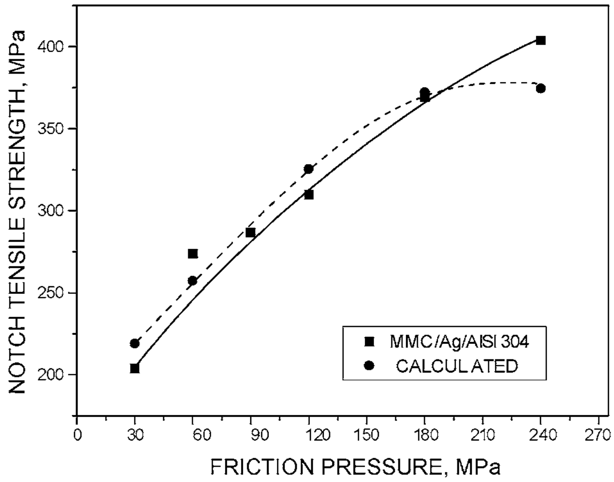

Figure 13 Calculated and measured notch tensile strengths in dissimilar MMC/Ag/AISI 304 stainless steel friction joints. Friction time, 4 s; forging pressure, 240 MPa; forging time, 1 s; rotational speed, 1500 rpm.

stress at which specimen failure will occur. A satisfactory failure criterion must consider both the material mechanical properties and the test specimen geometry. The present paper uses the failure criterion assumed by Teirlinck *et al.* when calculating notched tensile strength properties [18], i.e. it is assumed that failure occurs as result of void formation and void coalescence in the MMC substrate and this requires calculation of the volume change parameter D prior to calculating the failure stress. In this connection the observation of ductile failure on the fracture surfaces of tensile test specimens from MMC/Ag/AISI 304 stainless steel friction welds provides strong support for the assumption that the mechanical properties of the MMC material immediately adjacent to the joint interface have an important influence on the joint strength [14].

The volume change parameter D is determined by the relation [18]:

$$D = 0.56 \sinh \frac{3}{2} \frac{\sigma_m}{\sigma_y} \tag{9}$$

The triaxiality factor (σ_m/σ_y) in Equation 9 can be obtained either analytically (using Equation 8) or numerically. However, since MMC/Ag/AISI 304 stainless steel and MMC/AISI 304 stainless steel welded welds involve dissimilar materials as well as softened zone formation in the MMC substrate, the application of an analytical solution (Equation 8) would greatly oversimplify the problem. For this reason the triaxiality factor was calculated using FEM and the failure stress was subsequently calculated using the relation:

$$\sigma_{NF} = \left[\frac{1.28}{1 + D}\right]^m \sigma_{UT} \tag{10}$$

where, σ_{NF} = failure stress in notched tensile specimens, MPa, σ_{UT} = failure stress in unnotched tensile specimens, MPa, m = strain hardening index of the MMC base material

Figs 12 and 13 show that the calculated and actual notch tensile strength values. It is apparent that the calculated values closely correspond with actual tensile strengths of both dissimilar MMC/AISI 304 stainless steel and MMC/Ag/AISI 304 stainless steel friction welds. A detailed example describing the approach used to calculate the notched tensile strength of a dissimilar MMC/Ag/AISI 304 stainless steel weld is presented in the Appendix.

4. Discussion

Fig. 7 shows that the width of the softened zone region formed immediately adjacent to the dissimilar joint interface decreases when higher friction pressures are used during both MMC/AISI 304 stainless steel and MMC/Ag/AISI 304 stainless steel friction welding. However, increased friction pressure during welding also decreases the width of the intermetallic layer formed at the dissimilar joint interface [1]. The problem, therefore, is one of separating the effects produced by softened zone regions and by intermetallic layers on the mechanical properties of these dissimilar welds. Both factors have previously been used to explain the observed variations in weld mechanical properties. For example, a number of investigators have suggested that the mechanical properties of dissimilar friction welds are markedly decreased when the width of the intermetallic layer formed at the bondline exceeds a critical value [2–4, 19–21]. Also, the critical intermetallic layer width depends on the mechanical properties of the adjoining substrates [21]. Critical intermetallic layer widths range from 0.2 to 1.0 μm, although much higher critical values have been found in dissimilar diffusion welds [22]. For example, the notch tensile strengths of Al/Ti diffusion welds were only detrimentally affected when the intermetallic layer width exceeded 200 μm [22]. It is worth noting that intermetallic layer dimensions rather than intermetallic layer chemistry or mechanical properties constitutes the main emphasis in published research. It is assumed *per se* that the inadequate mechanical properties of intermetallic layers formed at the dissimilar joint interface will have an over-riding effect in promoting weld failure at this location. It is tacitly assumed that the mechanical properties of material immediately adjacent to the joint interface will not be important. However, this assumption will not be valid when age-strengthened aluminium alloys are friction welded. For example, a detailed investigation of the factors determining the mechanical properties of Al 6061/Al 6061 friction welds confirmed that the improved tensile strengths produced in welds made using high friction pressures resulted from the formation of narrow softened zones adjacent to the bondline. The widths of the softened regions produced in welds produced using very high friction pressures were small enough that the notch tensile strengths of completed joints were similar to those of the as-received Al 6061 T6 base material [5]. Consequently, it would be expected that the tensile strength properties of dissimilar MMC/AISI 304 stainless steel friction welds made using high friction pressures would be higher simply as a result of the formation of narrower softened regions in MMC base material immediately adjacent to the dissimilar joint interface.

Interlayer materials are generally introduced to prevent intermetallic layer formation at the dissimilar joint interface. When an interlayer is used and inhibits intermetallic layer formation, the mechanical properties of MMC/X/AISI 304 stainless steel friction joints will be improved when joints are made using high friction pressures. However, in the present study, the presence of a silver interlayer in MMC/AISI 304 stainless steel friction welds *of itself* promotes intermetallic layer formation at the dissimilar joint interface [14]. The mechanical properties of MMC/Ag/AISI 304 stainless steel friction joints therefore depend on the characteristics of i) the softened zone formed in the MMC substrate (its mechanical properties and width) and ii) the intermetallic layer formed at the dissimilar joint interface (its chemistry, dimensions, and mechanical properties).

In the present investigation the notch tensile strength of dissimilar friction welds was calculated based on the assumption that softened zone formation in MMC material immediately adjacent to the bondline is the critical factor that determines notch tensile strength properties. Using this assumption, the differences between the calculated and actual joint strengths ranged from 10 to 30 MPa in MMC/AISI 304 stainless steel welds produced using friction pressures from 120 MPa to 240 MPa, see Fig. 12. Dissimilar MMC/AISI 304 stainless steel welds produced using low friction pressures had wide softened zones (see Fig. 7), e.g. the softened zone width was 17.4 mm in a joint produced using a friction pressure of 30 MPa. Since this width exceeded the half of the gauge length of the notched tensile specimen (31.8 mm in Fig. 2), the influence of softened zone width on the mechanical behaviour of the MMC/AISI 304 stainless steel friction welds is determined by the mechanical properties of MMC material close to the bondline.

The actual and calculated notch tensile strength properties of MMC/Ag/AISI 304 stainless steel friction welds were in excellent agreement (see Fig. 13). For example, the softened zone width was 3.81 mm in a dissimilar MMC/Ag/AISI 304 stainless steel weld produced using a friction pressure of 180 MPa, while that in a weld produced using a friction pressure of 240 MPa was 3.48 mm. The difference in microhardness values in the softened zones of these welds close was 4 HVN and corresponds with a yield strength difference of 12 MPa (using Equation 2). The notch tensile strengths in actual welds differed by 11.1 MPa (see Fig. 3). Consequently, the difference in tensile strengths of these welds can be accounted for by the small increase in hardness (yield strength) in the softened zone, not by a change in softened zone width. However, this is not the case when the tensile strength of MMC/Ag/AISI 304 stainless steel welds produced using friction pressures from 120 MPa and 180 MPa are compared. In this case, the hardness difference in the softened zone was 3 HVN (see Fig. 8A) and this corresponds with a yield strength difference of 9 MPa. Since the actual tensile strength difference was around 60 MPa in these welds this mechanical property difference resulted from a decrease in softened zone width from 5.43 mm to 3.81 mm.

5. Conclusions

The mechanical properties of dissimilar MMC/AISI 304 stainless steel friction welds with and without silver interlayers were examined. The principal conclusions are as follows:

1. The notch tensile strengths of MMC/AISI 304 stainless steel and MMC/Ag/AISI 304 stainless steel friction welds increased when high friction pressures were applied during the joining operation. However, the highest notch tensile strength properties were obtained in MMC/Ag/AISI 304 stainless steel friction joints. The higher notch tensile strengths of dissimilar MMC/AISI and MMC/Ag/AISI 304 stainless steel friction welds resulted from the formation of narrow softened zones in MMC material immediately adjacent to the bondline, which decreased the equivalent stress and total equivalent strain values so that higher applied loads were required to cause joint failure during notch tensile testing.
2. The influence of softened zone width and hardness (yield strength) on the notch tensile strengths of dissimilar welds was analysed using finite element modelling. FEM in combination with the assumption of a ductile failure criterion was used to calculate the notch tensile strengths of dissimilar joints. The key assumption in this work is that dissimilar weld failure wholly depended on the characteristics (mechanical properties and dimensions) of the softened zone formed in MMC material immediately adjacent to the bondline. The modelling results produced based on this assumption closely correspond with the actual notch tensile strengths of dissimilar MMC/Ag/AISI 304 stainless steel and MMC/Ag/AISI 304 stainless steel friction welds. In welds made using low friction pressure, the mechanical properties of MMC material immediately adjacent to the bondline have a dominant influence on the notch tensile strength properties of completed joints. When joints are made using high friction pressures the softened zone width has the dominant influence on the notch tensile strengths of completed welds.

TABLE A1 Hardness and calculated yield strength values in the softened zone of a dissimilar MMC/Ag/AISI 304 stainless steel produced using a friction pressure of 240 MPa

Area	1	2	3	4	5	6	7	8
HVN	94.0	91.8	86.2	88.9	100.0	107.5	112.4	117.5
σ_Y	223.5	217.1	200.0	208.4	241.4	263.9	278.6	294.0

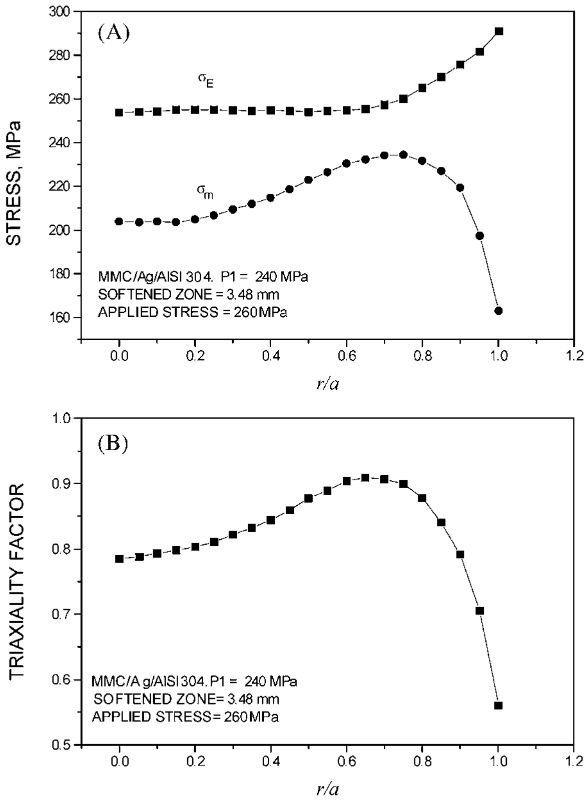

Figure A1 Stress and triaxiality factor distributions along a line located at 0.125 mm from the bondline. For an applied stress of 260 MPa. The calculated notch tensile strength was 374.4 MPa.

Acknowledgements
C. Maldonado wishes to acknowledge the financial support from the Consejo Nacional de Ciencia y Tecnología (México) and Universidad Michoacana de San Nicolás de Hidalgo (México).

Appendix: Notch tensile strength calculation
The procedure used when calculating the notch tensile strength of dissimilar MMC/Ag/AISI 304 stainless steel friction welds produced using a friction pressure of 240 MPa is explained in detail below. In this particular friction weld, the 3.48 mm wide softened zone was divided into eight rectangular areas, which extended from the centre to the periphery of the tensile specimen, see Fig. 3. These rectangular areas had heights of 0.5 mm. The microhardness values and the calculated yield strengths of the softened zone are indicated in Table A1. These yield strength values were used as input material properties in the finite element program.

The finite element model subjects a tensile load applied on the upper edge of the model and the applied load increases from 0 to 400 MPa in steps of 4 MPa. The effective stress and the triaxiality factor are calculated along a line parallel to the bondline at a distance of 0.125 mm from the bondline. This particular location was selected since ductile failure was observed in MMC material close to the bondline in dissimilar MMC/Ag/AISI 304 stainless steel and MMC/AISI stainless steel friction welds.

Fig. 1A shows the equivalent stress, hydrostatic stress and triaxiality factor distributions in a weld specimen produced using a friction pressure of 240 MPa. The failure condition was attained when a load of 260 MPa was applied during FEM modelling. The triaxiality factor is 0.91 at $r/a = 0.7$ in Fig. A1 and substitution of this value into Equation 9 produces a volume change parameter, $D = 1.043$. The softened zone hardness was 94 HVN (see Fig. 8A) and substitution of this hardness value into Equation 3, the unnotched failure stress (σ_{UF}) is 279.7 MPa. Substituting the unnotched failure stress into Equation 10 with $m = 0.075$ produces a notched failure stress, $\sigma_{NF} = 270.01$ MPa. This failure stress is attained in the region close to the bondline when the applied load is 260 MPa. Consequently, the notch tensile strength will be 374.4 MPa (1.44X the applied load of 260 MPa) during notch tensile testing.

References

1. C. MALDONADO and T. H. NORTH, 2000, preprint.
2. S. ELLIOT and E. R. WALLACH, *Met. Const.* **13**(3) (1981) 167.
3. *Idem.*, *ibid.* **13**(4) (1981) 221.
4. T. J. JESSOP, E. D. NICHOLAS and W. O. DINSDALE, in Proc. Conf. of Advances in Welding Processes, Harrogate, UK, May 1978, TWI, 23.
5. K. UENISHI, Y. ZHAI, T. H. NORTH and G. BENDZSAK, *Weld. J.* **79**(7) (1999) 184s.
6. E. A. ALMOND, D. K. BROWN, G. J. DAVIES and A. M. COTTENDEN, *Int. J. of Mech. Sci.* **25**(3) (1983) 175.
7. G. A. HENSHALL, R. S. ROSEN, M. E. KASSNER and R. G. WHIRLEY, *Weld. J.* **69**(9) (1990) 337s.
8. S. B. DUNKERTON, Report 201/1982, TWI, Abington Hall, Cambridge, 1982.
9. *Idem.*, Report 229/1982, TWI, Abington Hall, Cambridge, 1983.
10. J. W. DINI, W. K. KELLEY, W. C. COWDEN and E. M. LOPEZ, *Weld. J.* **63**(1) (1984) 26s.
11. H. HARTWIG and J. S. KOUPTSIDIS, in Proc. 7th Int. Vaccum Cong. and 3rd Conf. on Solid Surfaces, Vienna, Osterreichsche Sutdeingesellschaft fur Atomenergie, 1977, Vol. 1, p. 259.
12. J. W. HANCOCK and A. C. MACKENZIE, *J. of Mech. and Phys. of Sol.* **24** (1976) 147.
13. E. M. MIELNIK, in "Metalworking Science and Engineering" (McGraw-Hill, New York, N.Y., 1991).
14. C. MALDONADO, Y. ZHAI and T. H. NORTH, *Sci. and Tech. of Weld. and Join.* **3**(5) (1998) 213.
15. O. R. MYHR and O. GRONG, *Acta Metall. et Mater.* **39**(11) (1991) 2703.
16. M. HVAL, C. THAULOW, J. H. LANGE, S. H. HOYDAL and Z. L. ZHANG, *Weld. J.* **77**(5) (1998) 208s.
17. M. E. KASSNER, M. C. TOLLE, R. S. ROSEN, G. A. HENSHALL, G. A. and J. M. ELMER, "The Metal Science of Joining" (TMS, 1992).
18. D. TEIRLINCK, F. ZOK, J. D. EMBURY and M. F. ASHBY, *Acta Metall.* **36**(5) (1988) 1213.
19. A. FUJI, T. H. NORTH, K. AMEYAMA and M. FUTAMATA, *Mat. Sci. and Tech.* **8**(4) (1992) 219.
20. A. FUJI, T. H. NORTH, M. KIMURA and K. AMEYAMA, *Mat. Sci. Res. Int.* **1**(3) (1995) 188.
21. A. FUJI, K. AMEYAMA, T. H. NORTH and M. KIMURA, *ibid.* **1**(3) (1995) 193.
22. H. SUZUKI, N. UEHARA, A. NOZUE and T. OKUBO, in "Metallurgy and Technology of Practical Titanium Alloys," edited by S. Fujishiro, D. Eylon and T. Kishi (TMS, 1994) p. 239.

Received 6 November 2000
and accepted 11 December 2001